

## Computational Analysis of Cooling Effect with Different Flow Injection Angles On Double Chamber Model

Tao Xu, Zheng-Lei Yu and Jun-Lou Li

College of Mechanical Science and Engineering, Jilin University, Changchun 130025, P.R. China

**Abstract:** In order to explore a better cooling performance of transition piece, a numerical simulation is performed in this study. Advanced gas turbines are designed to operate at increasingly higher inlet temperatures to enhance efficiency and specific power output. This development in the operating temperature is enabled by advances in high-temperature resistant materials and by the development of effective cooling methods that lower the temperature of all surfaces that come in contact with the hot gases. Thus, there is a need for new cooling techniques or enhancing the current techniques available. The current study is a numerical simulation of film cooling in a double chamber model, which could simulate the Transition Piece's (TP) structure and performance. The adiabatic wall temperature and flow cooling effectiveness for the coolant injection angles (seven orientations, 90°, 75°, 60°, 45°, 30°, 15° and 0°) were investigated numerically. Fluent, a commercial CFD software, is extensively used in the current study for numerical simulations.

**Keywords:** Concave surfaces, cooling effectiveness, film cooling

### INTRODUCTION

Transition Piece (TP), primarily consisting heavier walls, single-piece aft ends, ribs, seal arrangements, selective cooling etc., is one of the hottest parts of a combustor of gas turbine. Increased combustor exit temperatures result in improved gas turbine efficiency and reduced fuel consumption. The new transition piece features a rounded body shape that balances the heat transfer loading both internally and externally and eliminates resonant frequency concerns (Fig. 1). It has an upstream aperture for the gas flow (which is cylindrical) and it is used to receive the gas flow directly from the corresponding combustion liners with a high level of enthalpy, they are conjured in a longitudinal direction so that their downstream ends comprise arched segments to form a ring-type configuration which opens toward the first stage of the gas turbine (stator). The working temperature of the TP is about 1200K to 1600K, which is very high for the material to withstand. Although, the mechanical stresses experienced by the TP are within acceptable limits compared to other parts, high temperatures and large temperature gradients affect the structural integrity of these components, which makes it a very critical component of a combustor in structural and thermal designs. Film cooling is a traditional method of cooling the inner surface of a TP (Xu *et al.*, 2012).

Therefore, over the past decades, many studies have devoted significant efforts to the development of

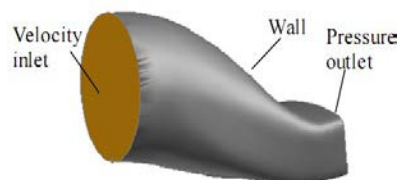


Fig. 1: Transition piece solid model

effective cooling schemes (Eriksen and Goldstein, 1974; Goldstein *et al.*, 1974). Internal convection, jet impingement and external film cooling or their combinations are available cooling techniques applied to turbine airfoil cooling. Internal cooling occurs where secondary cooling air passes through internal flow passages, which decreases the material temperature of the airfoil by conduction. Film cooling occurs by injecting the cooling air from tiny holes onto the airfoil surface, which forms a thin thermal insulation against hot gases.

As computational fluid dynamics becomes more widely used and more accepted as a design and analysis tool, it becomes increasingly more important to be able to assess its accuracy and its range of applicability. Computational fluid dynamics studies of film cooling have met with varying degrees of success. This issue describes an effort that uses the Fluent, Version 6.1.22, with second-order upwind differencing and three eddy-diffusivity turbulence models: realizable k- $\epsilon$ , Shear-Stress Transport (SST) and Spalart-Allmaras (S-A), to

compute two film cooling configurations for which experimental data are available to assess the accuracy of the computed results (Yakhot and Orszag, 1986; Shih *et al.*, 1995). One configuration is film cooling of a flat plate in which the coolant is injected from a plenum through one row of inclined circular holes. However, the effect of jet pulsation on the film cooling characteristics hasn't been studied extensively. Therefore it is important to investigate pulse frequency, blowing ratio and film hole geometry effects on film cooling, in order to identify under which conditions jet pulsation helps to increase film cooling effectiveness compared to the steady blowing and explain the flow physics behind that.

Most of the above works are based on film cooling in the flat surface. In real applications, a curved surface may be encountered. Walters and Leylek (2000), Berhe and Patankar (1999) and Garg and Gaugler (1997) conducted several CFD simulations of thermal-flow problems to understand the mechanism that governs film-cooling performance over a flat plate, a constant-curvature surface and a real film-cooled blade. In this issue, the model like a quarter torus with the curved double chambers is simulating the structure of transition piece, which has rarely mentioned in most studies. Our objective to make this simulation is to obtain a suitable injection angle, which is an important factor to improve cooling performance. The remainder of this study is organized as follows. Firstly, the film cooling problems studied are described. This is followed by the formulation, the numerical method of solution, the grid and the computed results. Subsequently, the effects of injection angle on film cooling through three rows of holes on a convex surface is studied.

### PROBLEM DEFINITION

**CFD model and boundary conditions:** The discrete coolant jets, forming a protective film chamber on the side of transition piece, are drawn from the upstream compressor in an operational gas turbine engine. The coolant flows fed through internal passages with surface holes. From the supply plenum, the coolants ejected through several rows of discrete-holes over the external boundary layer against the local high thermal conduction on the other side of the TP. This study builds a model, a fourth cylinder, which could simulate the TP's structure and performance, to discuss the effect of the type of the hole's angular location and the coolant injection angle on the film-cooling effectiveness over a concave surface. Figure 2 depicts computational film-cooling concave model and the injection holes. The distinction between concave models is in the hole's angular location.

A schematic of the flow domain along with boundary conditions and dimensions is given in Fig. 2.

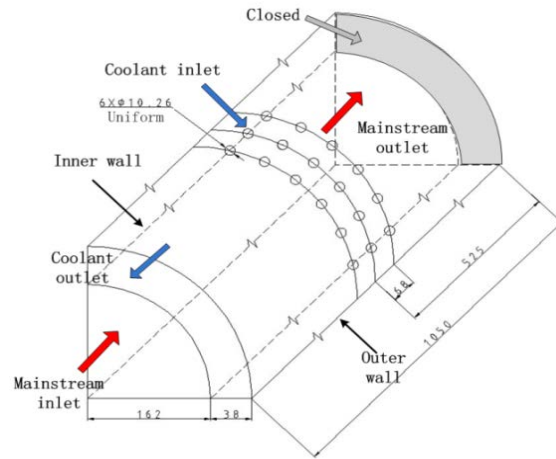


Fig. 2: Computational domain showing boundary conditions

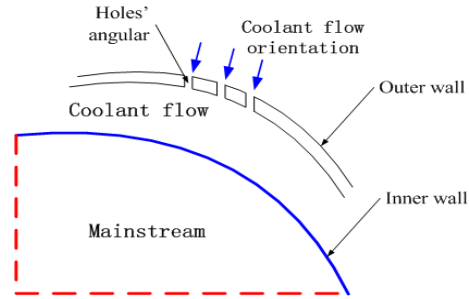


Fig. 3: The model with film hole geometry

As shown in figure, the fourth cylinder model has two chambers with length of 1050mm and the outer and inner radius is 200 and 162 mm, respectively. The outer chamber in the pic is called coolant chamber as the side is closed. Contrarily, the inner chamber goes by the name of mainstream chamber as the gas could through it from one side to another. There is a total of 18 holes uniformed distribution in three rows on the surface of the outer wall and the distance between the two rows of the holes is 68 mm. The size of all the holes is about 10.26 mm.

Boundary conditions were applied to specific faces within the domain to specify the flow and thermal variables that dictate conditions within the model. They are a critical constituent to the simulation and it is important that they are specified appropriately. Boundary conditions are first applied in Gambit, before exporting the mesh film to Fluent.

Figure 2 shows the quarter torus and its boundary conditions used for the modeling. Respectively, the cooling air and gas is coursing along the cooling chamber and the mainstream chamber with the the opposite direction. In the cooling chamber, the simulation is performed using air as the cooling fluid, velocity and temperature contours are set on the jet holes, pressure on the exit mouth. In another chamber,

assume that the mainstream is a mixture of O<sub>2</sub>, H<sub>2</sub>O, CO<sub>2</sub>, N<sub>2</sub>, as well as some rare gas and their ingredients are installed with 9%, 8%, 13%, 69%, 1%, respectively. Gas velocity and temperature contours are set on the surface of the sector section, pressure on the exit mouth and natural convection on the outside wall of the model are considered as boundary condition (Alfaro-Ayala *et al.*, 2011). The assumption of the solid wall of the quarter torus is modeled with a hypothesis of negligible thermal resistance by conduction, the thermal properties of the material were considered by Nimonic263, which could refer to the internet.

Figure 3 shows the model with film hole geometry used in this study. The figure shows the hole angle and the coolant injection angle. There are six holes of 10.26mm diameter in each row. For the analysis, velocity of the coolant flow is set at 6 m/s. The temperature of the coolant and mainstream flow are set as 300K and 1600K, respectively. In this study, 90° hole angle with different coolant injection angles were studied.

Table 1 shows a summary of the boundary conditions in the quarter torus and thermal properties of the fluid, respectively.

Meshing and simulation procedures: The computational domain incorporates the model, the HEXA module in the software, ICEM/CFD, used to generate the structured multi-block and the body-fitted grid system. This software allows separate grids to generated for different parts of the flow domain, using an appropriate grid system. In this study, the grid system associated with the parts of the main stream and the coolant supply plenum is H-type, while the surface of the inside wall and diversion lining are used the structured grids. Figure 4 shows the grids of the computational domain. The total number of the cells for the 3D domain is 271,000.

This study uses a commercial CFD code based on the control-volume method, FLUENT 6.1.22. The flow is treated as incompressible and steady state and the turbulence fluctuations are governed by the Boussinesq eddy-viscosity assumption. The standard k-ε turbulence model with the standard wall function is used to predict the flow structure and heat transfer over the film-cooling concave surface. The three-dimensional incompressible Reynolds-averaged Navier-Stokes equations are solved by a second-order upwind scheme unrelated to the convective terms, whereas the energy terms are evaluated using a third-order QUICK scheme. The coupling between velocity and pressure in momentum equations is governed by the SIMPLE scheme. The effect of buoyancy of the coolant jet is proposed by applying Boussinesq's approximation to the density. All runs were made on a PC cluster with four Pentium-4 2.8 GHz personal computers. The convergence criteria of the steady-state solution are judged by the reduction in the mass residual by a factor of 6, typically, in 2000 iterations.

Table 1: Boundary conditions

Component	Boundary conditions	Magnitude
Mainstream inlet	Mass flux rate	31.46 [kg/s]
	Gas temperature	1600 [K]
	Turbulent intensity	5 [%]
	Hydraulic diameter	0.324 [m]
Mainstream outlet	Pressure	1.512 [MPa]
	Turbulent intensity	5 [%]
	Hydraulic diameter	0.324 [m]
	Convection coefficient	10 [W/m <sup>2</sup> K]
Coolant chamber	Air temperature	300 [K]
	Pressure	1.4552 [MPa]
	Pressure recovery coefficient	0.95
	Turbulent intensity	5 [%]
	Hydraulic diameter	0.01026 [m]

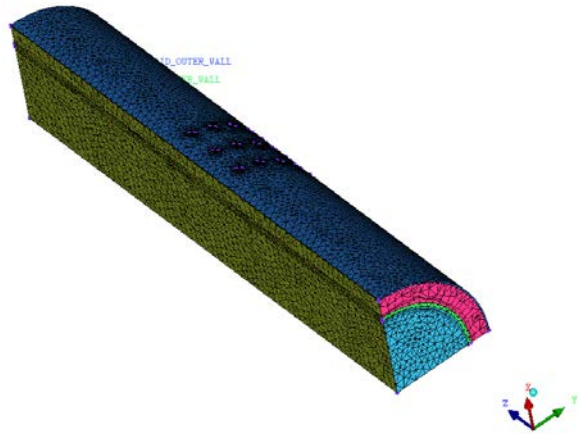


Fig. 4: Meshes

## NUMERICAL METHOD

The present film cooling study involves fluid which is steady, Newtonian, three-dimensional, incompressible and turbulent. Such fluid behaves according to three fundamental laws, namely the laws of continuity, conservation of momentum and conservation of energy. These laws are expressed as follows (Fluent Inc., 2003):

### Continuity equation:

$$\frac{\partial}{\partial x_i}(\rho u_i) = 0 \quad (1)$$

### Momentum equation:

$$\frac{\partial(\rho u_i u_j)}{\partial x_i} = -\frac{\partial P}{\partial x_i} + \frac{\partial \tau_{ij}}{\partial x_j} + \rho g_i + F_i \quad (2)$$

where P is the total pressure,  $\tau_{ij}$  is the stress tensor,  $\rho g_i$  and  $F_i$  are the gravitation body force and external body forces, respectively.

### Energy equation:

$$\rho(u_i \frac{\partial e}{\partial x_i}) = -\frac{\partial q_k}{\partial x_k} - p \frac{\partial u_k}{\partial x_k} + \phi \quad (3)$$

where,  $\phi$  is the viscous heat dissipation and the heat flux being given by Fourier's law.

$$q_k = -k \frac{\partial T}{\partial x_k} \quad (4)$$

**Turbulence model (k-ε):** The standard turbulence model is a semi-empirical model proposed by Launder and Spalding (1974), based on the model of the equations of transport for the turbulent kinetic energy ( $k$ ) and the dissipation rate ( $\epsilon$ ). This model is appropriate to study the turbulence in practical engineering flows due to its reasonable accuracy for a wide range of turbulent flows, the equations are defined as:

$$\frac{\partial}{\partial x_i}(\rho k u_i) = \frac{\partial}{\partial x_j}[(\mu + \frac{\mu_t}{\sigma_k}) \frac{\partial k}{\partial x_j}] + G_k + G_b - \rho \epsilon - Y_M \quad (5)$$

$$\frac{\partial}{\partial x_i}(\rho \epsilon u_i) = \frac{\partial}{\partial x_j}[(\mu + \frac{\mu_t}{\sigma_\epsilon}) \frac{\partial \epsilon}{\partial x_j}] + C_{1\epsilon} \frac{\epsilon}{k} (G_k) - C_{2\epsilon} \rho \frac{\epsilon^2}{k} \quad (6)$$

In these equations,  $G_k$  and  $G_b$  represent the generation of turbulent kinetic energy due to the mean velocity gradients and buoyancy, respectively.  $Y_M$  is the contribution of the fluctuating dilatation in compressible turbulence to the overall dissipation rate,  $C_{1\epsilon}$  and  $C_{2\epsilon}$  are constants. The turbulent (or eddy) viscosity  $\mu_t$  is computed by combining  $k$  and  $\epsilon$  as follows:

$$\mu_t = \rho C_\mu k^2 / \epsilon \quad (7)$$

**Equation of state:** The density varies according to the ideal gas law depending on the local pressure and temperature. The compressibility effect is accommodated during the simulation.

$$P = \rho RT \quad (8)$$

where,  $R$  is the gas constant.

**Thermodynamic equation:** The adiabatic cooling effectiveness ( $\eta$ ) is used to examine the performance of film cooling. The definition of  $\eta$  is:

$$\eta = \frac{T_m - T_{aw}}{T_m - T_c} \quad (9)$$

where,  $T_m$  is the mainstream hot gas inlet temperature, which is a fixed value for calculation the adiabatic cooling effectiveness of any location,  $T_c$  is the temperature of the coolant, which is assigned as a constant of 300K in this issue.  $T_{aw}$  is the adiabatic wall temperature. The value of  $\eta$  falls between from 0 to 1. When  $\eta = 0$ , it implies that the adiabatic wall temperature is equal to the hot gas temperature, which also suggests that the surface is under no film protection. On the other hand,  $\eta = 1$  means that the adiabatic wall temperature is the coolant temperature, which indicates complete film protection (Zakariya *et al.*, 2012).

## RESULTS AND DISCUSSION

In this section the results obtained with different hole angle location and the coolant injection angle are presented in order to validate the CFD model used to study pulsed jets film cooling physics. The main objective of this study is to investigate the cooling effects of film cooling and the temperature distribution in the inner wall. The temperature distribution is largely affected by the geometry, nature of the flow and temperatures of the flows at the inlets. As stated earlier, the mainstream temperature is set at 1300K for mainstream and 300K for coolant flow.

The minimum temperature distribution in the different cases is shown in Fig. 5. From the figure, it is seen that the temperature of the inner wall in different cases from 1384K to 1510K. The numerical values of minimum temperature in the model are connected the seven injection angles by line, which downtrend along with increased of injection angles.

Figure 6 shows a comparison of temperature distribution on the inner wall of the model, which is the conventional model in actual situations. This region will be the main region of concern in this study. The figure illustrates that the temperature at the starting

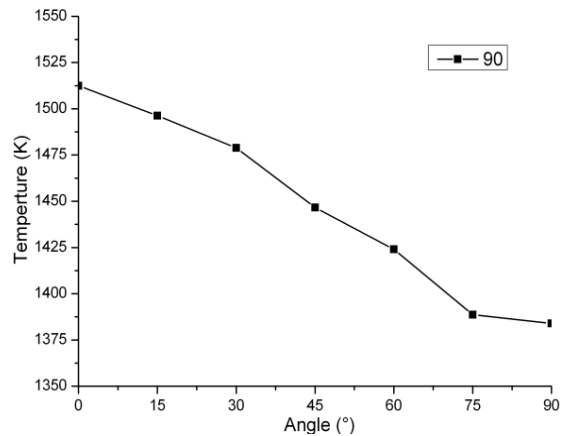


Fig. 5: Distributions of minimum temperature in the different coolant injection angles

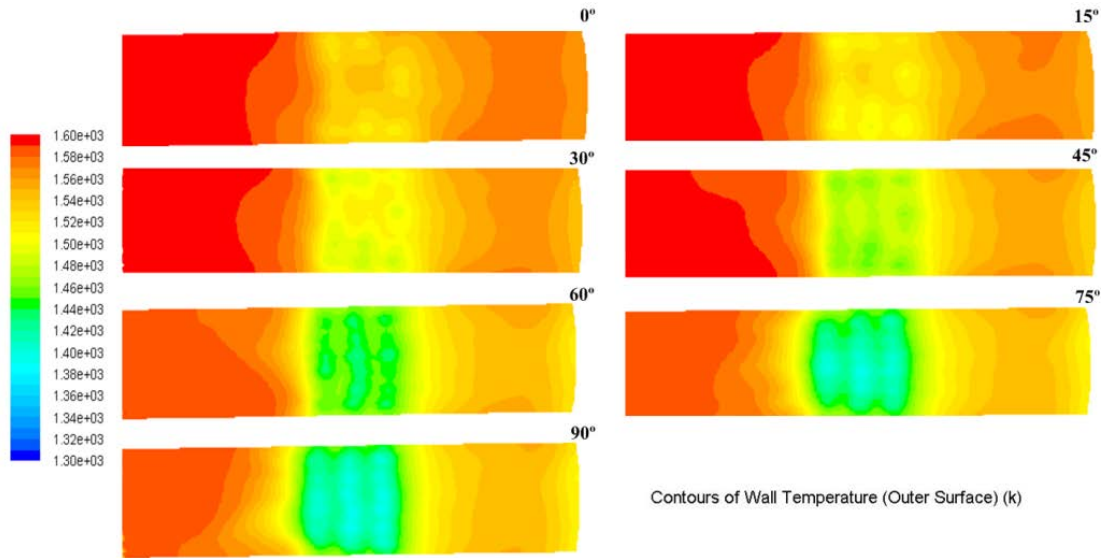


Fig. 6: Temperature contours at different coolant injection angles

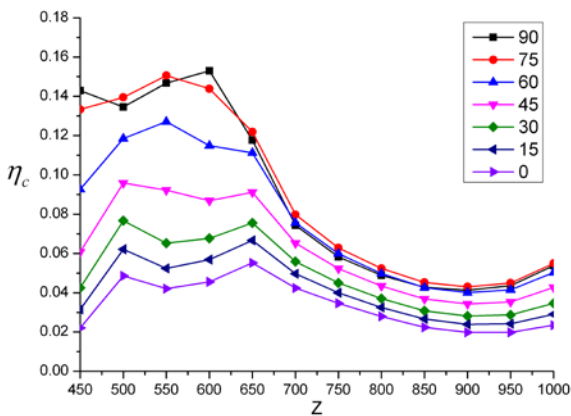


Fig. 7: Comparative analysis of cooling effectiveness at different coolant injection angles showing vortex induction towards the inner wall

point of the wall is high. It gradually decreases in the downstream. The starting point of the wall is cooled by the coolant holes at the curve  $Z = 450$  mm on the outer wall. Temperature is the same throughout the coolant holes. After the coolant strikes the inner wall, there are vortices formed. The jet impingement and the vortex formed out of the coolant flow cools the surface of the inner wall. The delicate color region (orange, yellow and green region) is approximately the region where the coolant strikes the inner wall after being reflected by the coolant holes, which the inner wall is cooled purely by film cooling. The coldest part is at the center of the domain ( $Z = 550$  mm). Though almost all flow in the coolant chamber is coolant flow, the cooling depletes along the  $Z$  axis, which is why there is a temperature rise in the region far from the impingement spot.

Film cooling performance is measured by the dimension parameter "adiabatic wall effectiveness ( $\eta$ )"

(Eq. (9)). For ideal case, the value of  $\eta$  is 1, i.e., when the adiabatic wall temperature is same as the coolant temperature. When there is no cooling, the value of  $\eta$  is 0.

Figure 7 presents averaged cooling effectiveness along the  $Z$  axis at different coolant injection angles ( $90^\circ$ ,  $75^\circ$ ,  $60^\circ$ ,  $45^\circ$ ,  $30^\circ$ ,  $15^\circ$  and  $0^\circ$ ) by color lines. In the picture, temperature and film cooling effectiveness are plotted against the distance along the inner wall. It is seen from the figure that the effectiveness is maximum between the  $Z = 500$  mm and  $650$  mm of the inner wall, which part is under the film region of the outer wall. In the coolant chamber, the flow is predominantly coolant flow and recirculation flow from the vortex that is formed out of the coolant flow. These flows have a low temperature and thus the effectiveness is high in this region. In the region far from the impingement spot., there is no new coolant injection for heat transfer between coolant and hot wall in the domain, which results in rise of the temperature of the inner wall. Thus, the effectiveness is reduced to below 0.03 in this region.

## CONCLUSION

A complete, three-dimensional numerical simulation of a film-cooled convex double chambers conducted to elucidate the coolant structure features that influence by film inclination and injection angle. The round cooling holes distributed in three rows. Comparisons are made to change flow injection angle on concave surfaces. Seven different angles of cooling flow are considered. During this investigation, enhanced flow injection angles are the reasons for the greater coolant of the transition piece structure. The methodology approach for this computational

prediction is validated using the existing experimental data and is successful.

#### ACKNOWLEDGMENT

This study is supported by Technology Development of Jilin Province (No.20096004) and Key Technologies R&D Program of Changchun (No.10KZ03).

#### NOMENCLATURE

$D_a$  = Diameter of coolant chamber  
 $D_g$  = Diameter of coolant chamber  
 $L$  = Length of the model  
 $T$  = Absolute static temperature  
 $X, Y$  = Non-dimensional coordinates in diameter,  
 $Z$  = Spanwise and mainstream directions

#### Greek symbols:

$\alpha$  = Hole angle  
 $\beta$  = Injection angle  
 $\eta$  = Film cooling effectiveness

#### Suffixes:

m = Mainstrataim flow  
c = Coolant flow  
aw = Adiabatic wall

#### REFERENCES

- Alfaro-Ayala, J.A., A. Gallegos-Muñoz, J.M. Riesco-Avila, A. Campos-Amezcuca, M.P. Flores-López and A. Mani-González, 2011. Analysis of the flow in the combustor-transition piece considering the variation in the fuel composition. *J. Therm. Sci. Eng. Appl.*, 3(2): 245-257.
- Berhe, M.K. and S.V. Patankar, 1999. Curvature effects on discrete hole film cooling. *J. Turbomach.*, 121: 781-791.
- Eriksen, V.L. and R.J. Goldstein, 1974. Heat transfer and film cooling following injection through inclined tubes. *ASME J. Heat Transfer*, 96: 239-245.
- Fluent Inc., 2003. *Fluent 6.3.26 Documentation*.
- Garg, V.K. and R.E. Gaugler, 1997. Effect of velocity and temperature distribution at the hole exit on film cooling of turbine blades. *J. Turbomach.*, 119: 343-351.
- Goldstein, R.J., E.R.G. Eckert and F. Burggraf, 1974. Effects of hole geometry and density on three-dimensional film cooling. *Int. J. Heat Mass Transfer*, 17: 595-607.
- Launder, B.E. and D.B. Spalding, 1974. The numerical computation of turbulent flows. *Comput. Method. Appl. M.*, 3: 269-289.
- Shih, T.H., W.W. Liou, A. Shabbir, Z. Yang and J. Zhu, 1995. A new  $\kappa - \epsilon$  eddy viscosity model for high Reynolds number turbulent flows. *Comput. Fluid.*, 24(3): 227-238.
- Walters, D.K. and J.H. Leylek, 2000. A detailed analysis of film cooling physics, Part I: Streamwise injection with cylindrical holes. *J. Turbomach.*, 122: 102-112.
- Xu, T., Z.L. Yu, W. Zhang, Z.M. Wang, J.L. Li and W.J. Zuo, 2012. Size optimization design of cooling structure in transition piece of gas turbine combustor. *J. Jilin Univ., Eng. Technol. Edn.*, 42(4): 863-866.
- Yakhot, V. and S.A. Orszag, 1986. Renormalization group analysis of turbulence 1: Basic theory. *J. Sci. Comput.*, 1(1): 3-51.
- Zakariya, M.K., M.S. Maher, N.A. Khalid and D.V. Regis, 2012. Heat transfer in magnetohydrodynamic fluid flows-A review. *Res. J. Appl. Sci. Eng. Technol.*, 4(15): 2412-2421.